LOWER HYBRID FREQUENCY HEATING IN TOROIDAL DEVICES WITH EMPHASIS ON WEGA RESULTS

G. TONON[+] - P. BLANC[+] - C. GORMEZANO[+] - W. HESS[+] -
G. ICHTCHENKO[+] - T.K. NGUYEN[+] - M. DURVAUX[+++] - R. MAGNE[+] -
W. OHLENDORF[++] - G. PACHER[++] - H. PACHER[++] - J.G.WEGROWE[++]

IPP 2/234 September 1977

MAX-PLANCK-INSTITUT FÜR PLASMAPHYSIK

8046 GARCHING BEI MÜNCHEN

MAX-PLANCK-INSTITUT FÜR PLASMAPHYSIK

GARCHING BEI MÜNCHEN

LOWER HYBRID FREQUENCY HEATING IN TOROIDAL DEVICES WITH EMPHASIS ON WEGA RESULTS

G. TONON[+] - P. BLANC[+] - C. GORMEZANO[+] - W. HESS[+] -
G. ICHTCHENKO[+] - T.K. NGUYEN[+] - M. DURVAUX[+++] - R. MAGNE [+] -
W. OHLENDORF[++] - G. PACHER[++] - H. PACHER[++] - J.G.WEGROWE[++]

IPP 2/234 September 1977

Invited contribution given at the 3[d] International Congress on Waves and Instabilities in Plasmas, PALAISEAU, (FRANCE), June 1977.

Published simultaneously as an EUR-CEA Report :
DPh-PFC-SIGn EUR-CEA-FC

[+] *ASSOCIATION EURATOM-CEA*
Département de Physique du Plasma et de la Fusion Contrôlée
Service IGn - Centre d'Etudes Nucléaires
85 X -38041 GRENOBLE CEDEX

[++] *MAX-PLANCK-INSTITUT FUER PLASMAPHYSIK*
GARCHING, Fed.Rep. of Germany

[+++] *E.R.M. BRUXELLES (Belgium)*

Die nachstehende Arbeit wurde im Rahmen des Vertrages zwischen dem Max-Planck-Institut für Plasmaphysik und der Europäischen Atomgemeinschaft über die Zusammenarbeit auf dem Gebiete der Plasmaphysik durchgeführt.

IPP 2/234 September 1977

LOWER HYBRID FREQUENCY HEATING IN TOROIDAL DEVICES WITH EMPHASIS ON WEGA RESULTS

G. TONON+ - P. BLANC+ - C. GORMEZANO+ - W. HESS+ - G. ICHTCHENKO+ - T.K. NGUYEN+
M. DURVAUX+++ - R. MAGNE+ - W. OHLENDORF++ - G. PACHER ++ - H. PACHER++ - J.G.WEGROWE++

+*ASSOCIATION EURATOM-CEA*
Département de Physique du Plasma et de la Fusion Contrôlée
Service IGn - Centre d'Etudes Nucléaires
85 X - 38041 GRENOBLE CEDEX

++*MAX-PLANCK- INSTITUT FUER PLASMAPHYSIK*
GARCHING, Fed. Rep. of Germany

+++*E.R.M. BRUXELLES (Belgium)*

ABSTRACT : Among the various methods of additional heating of toroidal magnetically confined plasmas by high frequency field, heating near the lower hybrid frequency appears promising. With principal reference to the results of the WEGA-TOKAMAK, complemented by results on analogous experiments, the discussion centers on three points : first, the coupling of the H.F. energy to the plasma ; secondly, the modifications induced in the plasma parameters and finally the ion heating by absorption of the H.F. energy.

INTRODUCTION.

It is usually recognized that a considerable amount of heating power, additional to the ohmic heating will be required to reach ignition in a reactor of the Tokamak or Stellarator type /1/. To this purpose, the injection of intense beams of energetic neutral particles as well as the use of R.F. fields are being currently investigated.

The latter category of methods has been the object of various studies (/2/, /3/, /4/). Among the considered methods, the use of R.F. waves in the neighbourhood of the lower hybrid resonance frequency (L.H.R) appears as one of the most interesting in view of reactor applications : due to this medium frequency (of the order of 1 GHz) coupling of energy by means of waveguides is already possible, thus avoiding many technical problems connected with (material) structures inside the vessel /5/, /6/, /7/, and the frequency is still in a range where large power will be available without difficult development.

Several experiments on plasma heating in toroidal devices have been undertaken or planned in the last few years. The parameters of existing (FT1, WEGA, ATC, ALCATOR) and planned (PDX, ASDEX, JET, JT60, FT) experiments on lower hybrid heating are plotted in Fig. 1 as a function of toroidal magnetic field and electron density. The accessible regions for lower hybrid heating are given for different frequencies (Ref. / 7 /. For example, WEGA in the present conditions (500 MHz, 15 kG) demands a density of the order of $2.10^{13} cm^{-3}$. It is to be noted that, with the exception of high-field machines (ALCATOR, FT) the frequency to be used in devices of the next generation is little different from the present experiments. On the contrary, the necessary power, now of the order of several hundred kW for 10 to 20 ms., will be of the order of several MW (CW) in the next generation.

In this paper we shall present some results of the L.H.R. heating studies through those obtained in the Tokamak WEGA^{++}, whose parameters are given in Table I.

1 - R.F. COUPLING AND WAVE PROPAGATION.

Both coupling by phased arrays of waveguides /10/ and internal launching structures /16/ have been used success fully. In all cases, the accessibility condition /8/, /9/ has been satisfied.

An excellent verification of the coupling theory of the Grill / 5 / has been obtained with two and four-elements Grills on the linear device H.1 and on A.T.C. (Fig. 2, reproduced from reference /10 /). In the figure, exceptional agreement between the experimentally determined and the theoretically predicted reflection coefficient as a function of the phase difference between succeeding guides is demonstrated (The theoretical values were calculated using the experimental density gradient at the plasma edge). In the A.T.C. experiment, the normal coupling was 70 to 80% and up to 95% with appropriate matching.

In WEGA, loops with coaxial feeders (Fig. 3) had to be used because of the small available port size. For these loops no coupling theory comparable to the Grill theory exists. The natural coupling was also 60 tc 70%, and transmission in excess of 95% was easily obtained by matching. Measurements with Langmuir probes have shown that the density at the radius of the coupling loops was a few times $10^{11} cm^{-3}$, well above the cutoff density at 500 MHz. This may influence the coupling between the loops. In fact, the natural reflection coefficient was, in this experiment, insensitive to the phase difference of the loops.

From measurements of the density gradient using Langmuir probes on the edge of the plasma and Thomson scattering further inside, one can trace the so-called resonance cones /11 / along which the H.F energy should propagate inside the machine. It is seen on the figure 4 that they make one to two revolutions around the device before reaching the linear conversion region. The dispersion relation is shown schematically on Fig. 5. According to the linear theory, the incident cold plasma wave should be transformed into a hot plasma wave at a density slightly less than the cold resonant density /12/, /6/. In this region of the turning point, linear absorption of the wave is expected. Non linear effects may occur along the wave path as the electric field increases.

The spectrum of parallel wave number $N_{//}$ in WEGA is estimated to extend from accessibility ($N_{//c} \sim 1.6$) to about 5 or 6. The conversion region has a finite radial extent as a function of the density, temperature and magnetic field profiles. This region is shown in Fig. 6. Here, the size of the hatched region corresponds to the width of the spectrum in $N_{//}$. It is noted that the asymmetry is due to the major radius dependance of the magnetic field. The exact location of the heating zone in minor radius therefore depends on the poloidal angle at which the resonance cone attains this region. Once heating has taken place, the temperature can be expected to become uniform along a magnetic surface.

2 - EFFECTS OF THE H.F. ON THE PLASMA PARAMETERS.

a) Fast Ion Tail.

As in other H.F. experiments, /13/ to /16/ on the application of the H.F to the WEGA plasma, an energetic ion tail appears (Fig.7). It has a mean energy of $\approx$1 keV, increasing to 2 keV at higher power levels /17/,/21/ Its decay time is normally very short after the end of the H.F. pulse, in our case less than or of the order of 100 µs. / 17 /.

An experiment has been performed in which a radial limiter of limited extent vertically was inserted near the H.F. loops but in the shadow of the main limiter / 17 /. The fast ion flux decreased as the plate approached the plasma, which can be interpreted as due to the decrease of the volume of poorly confined plasma between the fixed and the movable limiter (Fig. 8). This observation, together with the rapid decay time, led to the conclusion / 17 / that the fast ions come from the edge of the plasma. The corresponding power lost by these ions may be calculated to be several kilowatts on the (poorly justified) assumption that they are emitted isotropically in velocity and physical space. It is noted that charge exchange can only give information in a very narrow region of both spaces.

Another observation concerning the fast ion tail resulted from experiments at lower magnetic field (10 kG), at which neither the lower hybrid resonance nor the turning point exist in the plasma. Here, a fast ion tail was observed whose total flux was comparable with that observed under normal conditions. The fast ions are therefore not linked with the phenomenum of linear wave conversion. Conversely, their number seems to depend strongly on the electric field at the point of creation /17 /.

b) Density Increase.

In most experiments, the application of H.F. at appreciable power levels results in an increase in electron density. In WEGA, Thomson scattering (Fig. 9) shows that the profile is not strongly distorted by the application of H.F., but rather the density increases globally. Therefore, the peak density remains proportional to the average density measured by microwaves as a function of time (Fig. 10). The figure shows the time development for two H.F. power levels and several different pulse lengths. It is noted that the time rate of change is roughly proportional to the H.F. power and the total increase to the pulse length.(During the long pulses the HF power decreases in time due to the limited energy of the emitter power supply). To investigate the reason for the density increase, it is necessary to consider the type of ion responsible. From the analysis of soft X-rays, one obtains the electron temperature and, knowing the electron density from the interferometer it is then possible to estimate the concentration of one impurity, assuming it is dominant in the discharge, from the intensity of soft X-radiation /18 /.

One finds that the hypothesis of dominant oxygen impurity reflects well the experimental conditions for the plasma without H.F. During the H.F. pulse the total oxygen ion concentration in the central part of the plasma, deduced by this method, does not rise but instead seems to decrease slightly (Fig. 11). This tendency is confirmed by the evolution of the intensity of O VII line emission. Figure 12 shows this intensity normalized to the squared electron density, i.e. a quantity proportional to the O VII ion concentration.

It had therefore been concluded tentatively that the primary source of the density increase was ionization of background deuterium. To test this hypothesis, the fast gas valve was programmed to give a density evolution similar to that produced by the H.F. It is seen that the time evolution of the impurity concentration is similar (Fig.11,12).

The conclusion follows that, at the beginning, an appreciable portion of the density rise results from deuterium, although impurities may be added later on in the pulse. We should note here (Fig. 13) that the density profiles obtained during H.F. and those during the fast gas pulse are very similar.

c) Loop Voltage Increase.

The major macroscopic difference between the discharges using gas puffing and those with H.F. is the increase in loop voltage by 70-80% during the H.F. pulse, (Fig. 14), decreasing fairly rapidly at the end of the H.F. pulse. The shape of the voltage peak makes it appear unlikely that the measurement represents a inductive effect.

To explain the change in voltage , one could invoke a change in electron temperature. However, the peak temperature is observed not to vary appreciably. Equally, no drastic changes in temperature profile have been observed, although they cannot be excluded because of the large error bars on the measurement (Fig. 15). Alternatively one could explain a resistance increase by an increase in impurities. However, soft-X-measurements show no appreciable increase in Z_{eff}, which even shows a tendency to decrease slightly during the H.F. as deduced from the results shown in figures 11 and 12.

Thus, an increase of the resistance by an increase of impurities appears excluded, but neither a change in current density profile nor anamalous resistivity /19/ can be excluded.

3 - ION HEATING.

a) Numerical Simulation.

A simulation of the WEGA experiment has been run using the Fontenay code / 20/.

When 50 kW of localized energy are added to the ion species at about half the radius of the plasma (Fig. 16 a), localized heating is seen immediately. The ion temperature becomes uniform later in time. Thus, after 10 ms., considerable heating has taken place throughout the plasma volume. On the other hand, if deposition of energy takes place farther out on the plasma radius, such as 3/4 the limiter radius (Fig. 16 b), no effect is visible toward the interior because of the larger energy losses.

One obtains from the code the local concentration of oxygen ions six times ionized. From this, on multiplying by the local electron density and the appropriate excitation cross-section, one finds that the O VII line emission should be localized around half the plasma radius (Fig. 17).

b) Experimental results.

The result of a measurement by charge exchange appears on the figure 18 against time /21/. It must be pointed out that a reliable determination of ion temperature by charge exchange during the H.F. pulse is impossible because of the effect of the ion tail mentioned earlier. However, after the H.F. pulse, and after disappearance of the hot ion tail in 100 µs.,the temperature is seen to be clearly higher by 80 eV than that obtained by a D_2 puff programmed to give the same density increase as the H.F. In addition, the long decay-time of ion energy suggests that thermalization has taken place. From this decay and the evolution of the density one can estimate an H.F. power input of 25 to 50 kW to the ions if heating is uniform in volume /21 /. By comparison, the power given to ions by electrons is approximately 15 kW from the code. We note that, in our experiment, the long decay time is definitely not instrumental.

The second method of ion temperature measurement, using the Doppler broadening of the O VII line, works during the H.F. pulse and indicates also an appreciable temperature increase over that obtained with the programmed deuterium puff (Fig. 19). Like charge exchange, it indicates a temperature increase of 80 eV, indicating nearly homogeneous heating at least to half the plasma radius. These results are in agreement with the Fontenay code, where 50 kW power to the ions gave a temperature increase of 70 eV (Fig. 16 a) when the density increase is taken into account. Similar results on O VII line emission were observed on the A.T.C. device at the same H.F. power / 10 /. Furthermore, the ion temperature in A.T.C. deduced from C IV line emission (localized near the plasma edge) shows very little increase. / 10 /.

It is note worthy (Fig. 19) that the increase of temperature from the gas puff arrives very late in time simultaneously with the highest ion temperature reached during the H.F. To look at the behaviour of the ion temperature with density on figure 20 two series are shown giving the time evolution of electron density together with the ion temperature as measured by O VII line emission. The difference between the two sets of curves is in the density at the beginning of the H.F. and in the H.F. pulse length. Note that at higher density O VII shows a temperature increase starting almost immediately. For the case of lower starting density, the density first increases and, when it reaches the same value as in the first case, O VII again shows a temperature increase.

As far as saturation of the ion temperature measured by the O VII line is concerned, this again saturates at the same density for the two cases.

The tentative conclusion is that the heating does indeed depend on the absolute value of density, as predicted by the linear theory. As the density increases because of the H.F., the turning point moves outwards and heating is seen on the O VII signal when in both cases, the turning point is at about half the radius. A continued increase of density then pushes the turning point toward the outer region of the plasma where according to the code, losses are so high that no heating occurs toward the inside of the plasma. This could then be responsible for the observed saturation in the temperature.

4 - CONCLUSION.

The following points may be made on lower hybrid heating in toroidal machines.

1°) - Coupling by arrays of wave guides or loops has been used with success. Transmission in excess of 95% was easily obtained by matching.

2°) - No large scale perturbations of equilibrium due to H.F. have been observed.

3°) - Bulk plasma heating is observed with H.F. power absorbed by the ions of the order of twice as large as the power given to ions by collisions. For WEGA :

$$\frac{\Delta T_i}{T_i} \simeq 60\text{-}70\%$$

has been obtained with 180 kW applied H.F. power.

4°) - The value of the density plays a role in the heating processes. During the experiments at different starting densities in WEGA, heating has been observed only for densities for which the linear turning point is in the plasma.

5°) - Not yet understood are the reasons for the density increase, the mechanisms for the production of energetic ions and the effect of the H.F. on the loop voltage. Profile measurements are not yet sufficiently complete to determine the energy balance.

6°) - From the technical point of view, H.F. generators up to 500 kW are available, sufficient for present generation machines. Development of generators of the orders of 1 MW-CW seems possible at reasonable cost in the near future.

ACKNOWLEDGEMENTS.

The authors are very grateful to P.P. LALLIA, some of whose experimental work on charge exchange measurements has been included here to C. MAHN who performed the Thomson scattering measurements. The work of the WEGA technical staff (+) has been indispensable to obtain the results presented here. Furthermore, we would like to thank W. HOOKE of the Princeton Plasma Physics Laboratory for letting us quote the experimental results of Grill coupling, and F. WERKOFF, who ran the Fontenay code.

(+) - K. BENNYETOU* - J. BLANC* - M. BORREL* - F. BOURG* - J.J. CAPITAIN* - F. COULON* - R. FRITSCH** - W. GRAF** - D. KOEHLER** - M. LIPA* - J.R. MARTIN* - B. MOULIN* - D. MOULIN* - J.P. MOUSSY* - M. PAUME* - M. PETITJEAN* - M. PROVOST* - M. RAFFIN* - G. SENTIS* - G. SCHENK*.

REFERENCES.

/1/ - T. STIX, Symposium on Plasma Heating and Injection, Varenna September 21 - October 4 (1972).

/2/ - E. CANOBBIO "R.F. Heating of Fusion Reactor", Second Topical Conference on R.F. Plasma Heating, Lubbock, June 20-22 (1974), C1-1, Vol. 1.

/3/ - M.E. OAKES, Survey of Lower Hybrid Studies, Second Topical Conference on R.F. Plasma Heating, Lubbock, June 20-22 (1974), B-11, Vol. 1.

/4/ - T. CONSOLI, Third Symposium on Plasma Heating in Toroidal Devices, Varenna September 6-17 (1976), p. 11-20.

/5/ - M. BRAMBILLA, Nuclear Fusion 14, p. 327, (1974) ; Proc. of the VII European Conference Plasma Phys. and Controlled Fusion, Lausanne, Vol. II (1975) ; Nuclear Fusion 16, p. 47 (1976).

/6/ - P. LALLIA, Second Topical Conference on R.F. Plasma Heating, Lubbock, June 20-22 (1974), C-3.

/7/ - M. BRAMBILLA - P. LALLIA, T.K. NGUYEN, 3d International Meeting Theoretical and Experimental Aspects of Heating of Toroidal Plasmas, Grenoble (1976) Vol. II p. 283-304.

/8/ - T. STIX, The Theory of Plasma Waves, Ed. McGraw-Hill, New-York (1962).

/9/ - V. GOLANT, Sov. Phys. Tech. Phys. JETP 16, 1980 (1972).

/10/ - S. BERNABEI et al., Third Symposium on Plasma Heating in Toroidal Devices, Varenna, September 6-17 (1976) p. 68-78.

/11/ - H.H. KVEHL, Phys. Fluids 5, 1095 (1962).
R.K. FISHER and R.W. GOULD, Phys. Fluids, 14, 857 (1971).

/12/ - S.S. PESIC, Nuclear Fusion 11, p. 461 (1971) ; Plasma Physics 15, p. 193 (1974).

/13/ - J.P. GLADKOVSKY et al. Fifth European Conference on Controlled Fusion and Plasma Physics, Grenoble 21-25 August (1972), Vol. 2 p. 109.

/14/ - V.V. ALIKAEV et al. Sixth European Conference on Controlled Fusion and Plasma Physics, Moscou 30 July 4 August (1973), Vol. 1 p. 63.

/15/ - H. TAKAHASHI et al., Physical Review Letters 39, 1-31 (1977).

/16/ - P. BLANC et al. 3d International Meeting Theoretical and experimental Aspects of Heating of Toroidal Plasmas, Grenoble (1976), p. 251, Vol. II.

P. BLANC et al., 6th Conference on Plasma Physics and Controlled Nuclear Fusion Research, Berchtesgaden, October 6-13 (1976) IAEA CN-35G9.

P. BLANC et al., Congres National de Physique des Plasmas, PARIS, December 6-10 (1976), C3-155 (to be published).

/17/ - P. LALLIA - G.W. PACHER - H.D. PACHER, Third Symposium on Plasma Heating in Toroidal Devices, Varenna September 6-17 (1976), p. 79.

/18/ - S. VON GOELER et al., Nuclear Fusion 15, 301 (1975).

/19/ - V.V. PARAIL, JETP Lett. 24, 4, 175 (1976).

/20/ - Fontenay code MAKOKOT.

/21/ - J.G. WEGROWE et al., 8th European Conference on Controlled Fusion and Plasma Physics, Prague, September 19-23 (1977) (to be published).

TABLE I

WEGA[++] - TOKAMAK

1 - WEGA CHARACTERISTICS	
Large plasma radius	R_o = 72 cm
Minor plasma radius	a = 13 - 16 cm
Minor wall radius	a_W = 22 cm
Toroidal magnetic field	B_ϕ = 14,4 kG
2 - WEGA PLASMA characteristics without H.F.	
Deuterium plasma	
Plasma current	I_p = 45 - 60 kA
Ohmic heating power	P_Ω = 100 - 130 kW
Peak electron density	n_{eo} = 1 - $6.10^{13}cm^{-3}$
Peak electron temperature	T_{eo} = 500 - 1000 eV
Peak ion temperature	T_{io} = 150 - 250 eV
Energy confinement time	τ_{Ee} = 3 - 5 ms.
Z_{eff}	Z_{eff} = 2 - 6
H.F. HEATING WAVE PARAMETERS	
H.F. frequency	f = 500 MHz
Maximum H.F. power	P_{HF} = 200 kW
Maximum pulse duration	$\Delta\tau$ = 5-15 ms.
Parallel wave index	$N_{//}$ = 2 - 3

++ - WEGA is a common experiment built and run by the Commissariat à l'Energie Atomique and the Max Planck Institut für Plasmaphysik - Garching and is operated in France at Grenoble. The Belgian Ecole Royale Militaire also takes part in this common program.

FIGURE CAPTIONS.

Fig. 1 - Frequency ranges of interest for lower hybrid heating.

Fig. 2 - a) Schematics of a waveguide coupling system.
b) H.F. reflection coefficient and its comparison with theory (according to /10/, with kind permission of the authors).

Fig. 3 - The 2 loops coupling system used on WEGA.

Fig. 4 - H.F. both along the torus (WEGA) - Computation using the electron density profile as measured by Thomson Scattering and 3 Langmuir probes at the plasma edge.

Fig. 5 - Schematics of the dispersion relation.

Fig. 6 - The wave conversion zone of the linear theory in WEGA as a function of the peak electron density.

Fig. 7 - Energy spectra obtained by analysis of charge-exchanged neutrals before, during and ofter an H.F. pulse.

Fig. 8 - Detected neutrals flux at 3 keV as a function of the location of the movable limiter.

Fig. 9 - Density profile by Thomson scattering with H.F. on and without H.F.

Fig. 10- Behaviour of the peak electron density for efficient H.F. power and various pulse durations (microwave interferometry).

Fig. 11- Total concentration of ionized oxygen towards the center of the discharge in a standard discharge, in a discharge with H.F., in the simulation by gas puffing (as deduced from X-ray measurements).

Fig. 12- Estimate of O^{6+} concentration (from the intensity of O VII line) in the discharge with H.F., and in the gas puffing case.

Fig. 13- Density profiles during H.F. pulse and in the gas puffing case.

Fig. 14- Behaviour of the loop voltage during on H.F. pulse at 180 kW level and during gas puffing.

Fig. 15- Electron temperature profiles by Thomson scattering during H.F. and in a discharge without H.F.

Fig. 16- Code run with 50 kW assumed power coupled to be ions.
a) Power deposition around mi-radius.
b) power deposition at $r/a \sim 0.75$.
(The H.F. is on between 0 and 10 ms).

Fig. 17- Density of O^{6+} and radiation intensity of the O VII line as deduced from the code.

Fig. 18 - Ion temperature as deduced from charge exchange analysis in a discharge with H.F. ; as compared with the gas-puffing case (In the latter, the behaviour of the electron density during H.F. was closely. Simulated by a programmed injection of deuterium).

Fig. 19 - Ion temperature as deduced from the broadening of the O VII line in a discharge with a long H.F. pulse and in the corresponding gas-puffing simulation.

Fig. 20 - Correlation between electron density and heating during H.F. pulses.

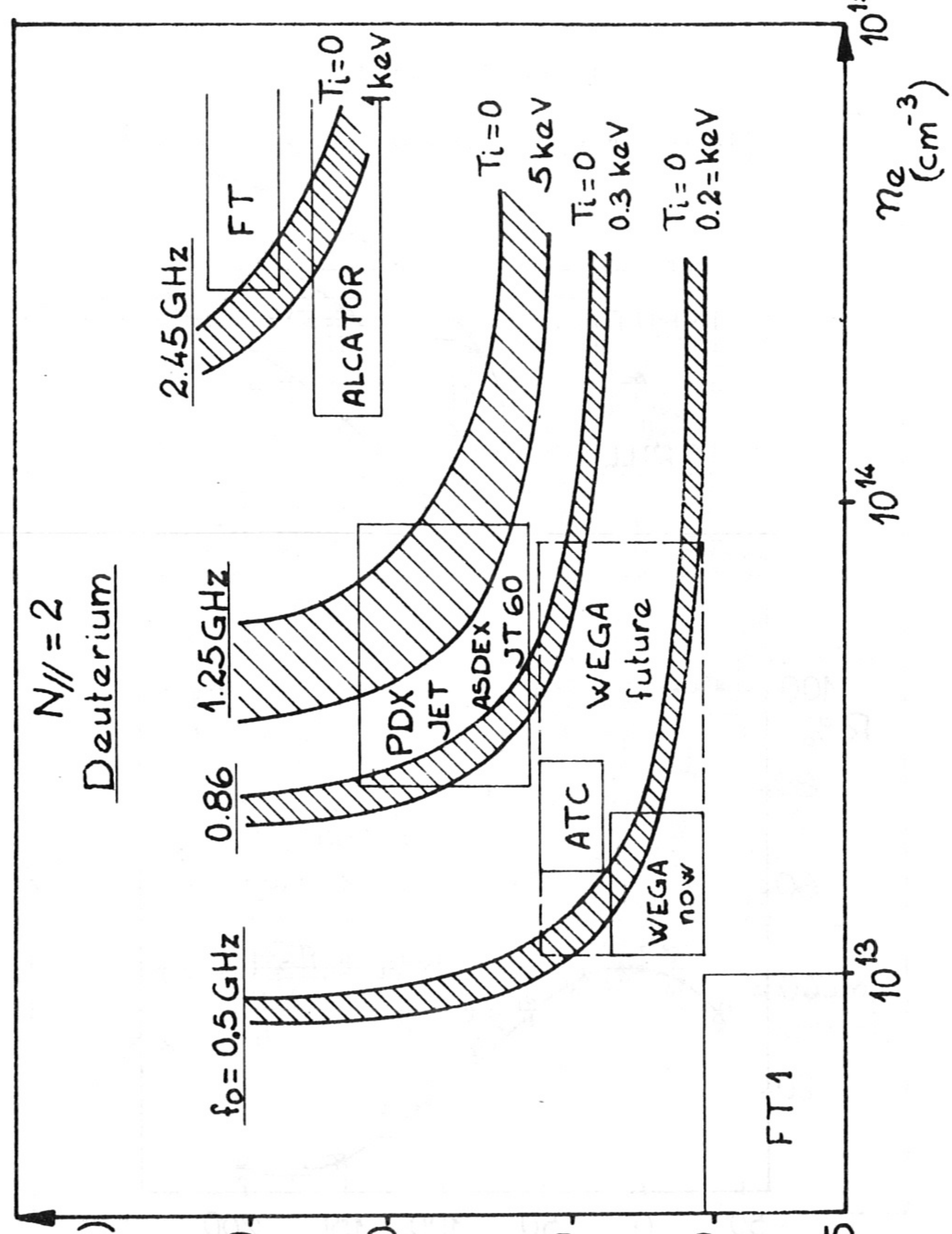

N// = 2
Deuterium
B (kg)
100
50
20
10
5
10^13
10^14
10^15
ne (cm^-3)
f0 = 0.5 GHz
0.86
1.25 GHz
2.45 GHz
FT
ALCATOR
PDX
JET
ASDEX
JT 60
WEGA future
ATC
WEGA now
FT 1
Ti = 0
1 keV
Ti = 0
5 keV
Ti = 0
0.3 keV
Ti = 0
0.2-keV

Fig. 1

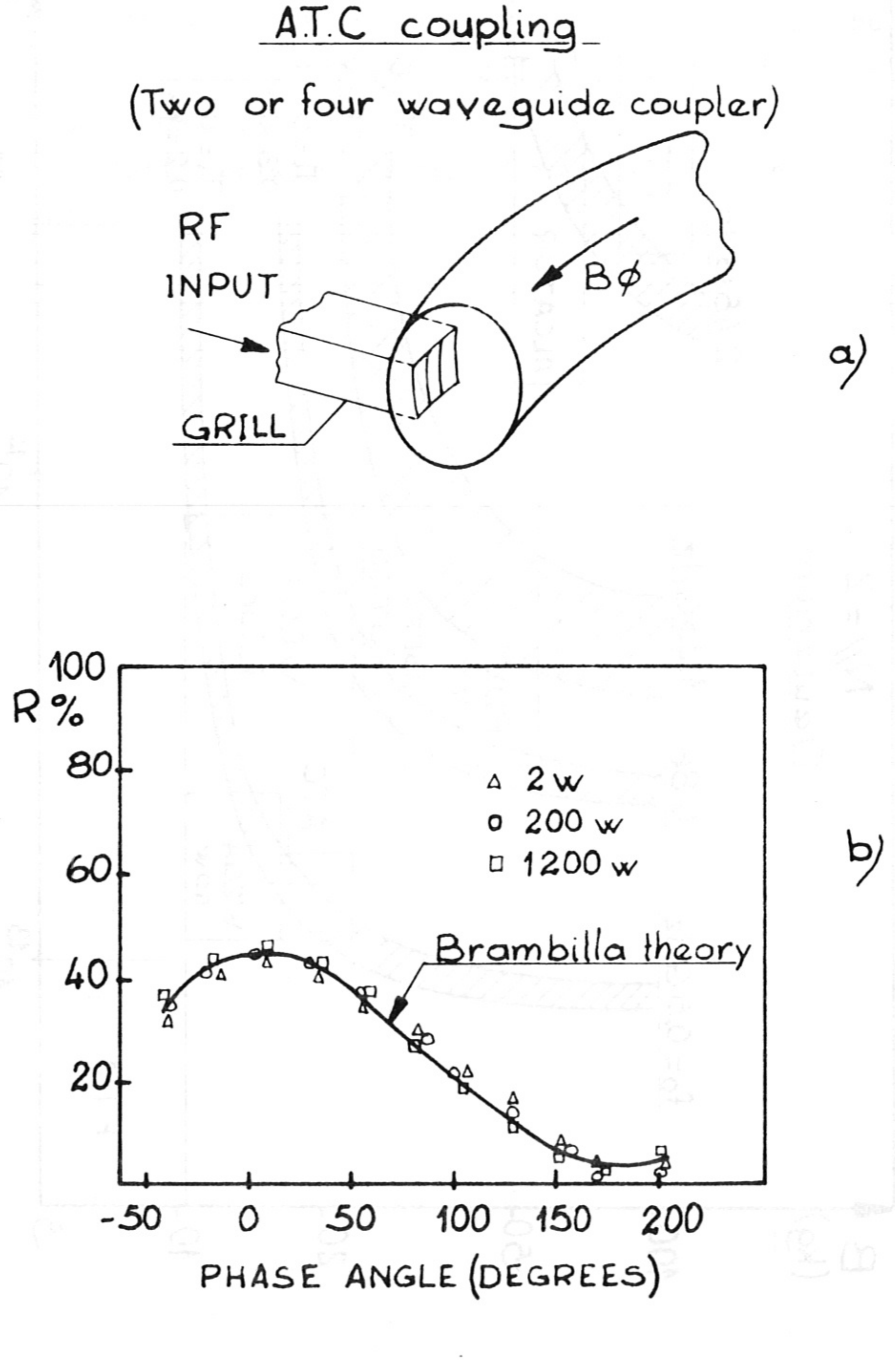
A.T.C coupling
(Two or four waveguide coupler)
RF
INPUT
GRILL
Bφ
a)
100
R %
80
60
40
20
2 w
200 w
1200 w
Brambilla theory
-50
0
50
100
150
200
PHASE ANGLE (DEGREES)
b)

Fig. 2

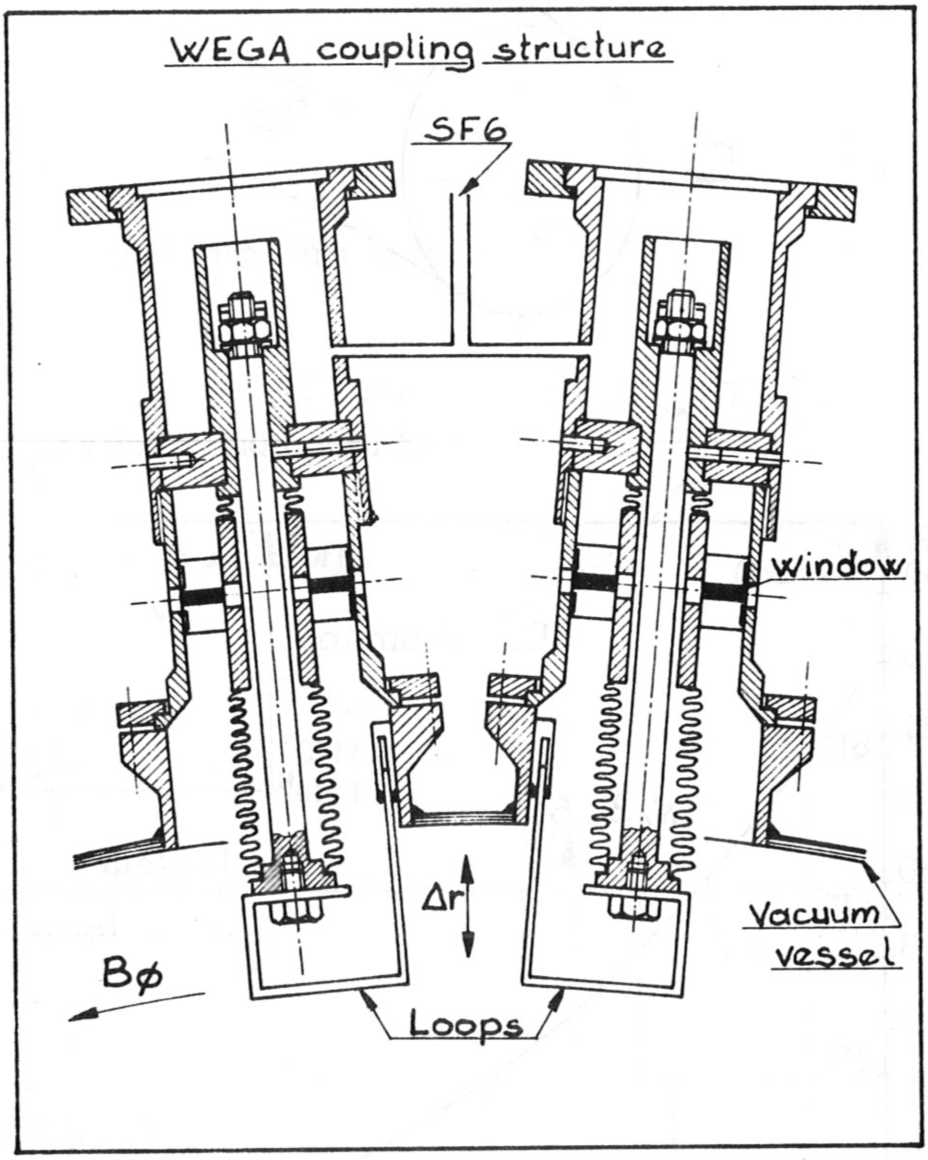
WEGA coupling structure
SF6
Window
Vacuum
vessel
Δr
Bϕ
Loops

Fig. 3

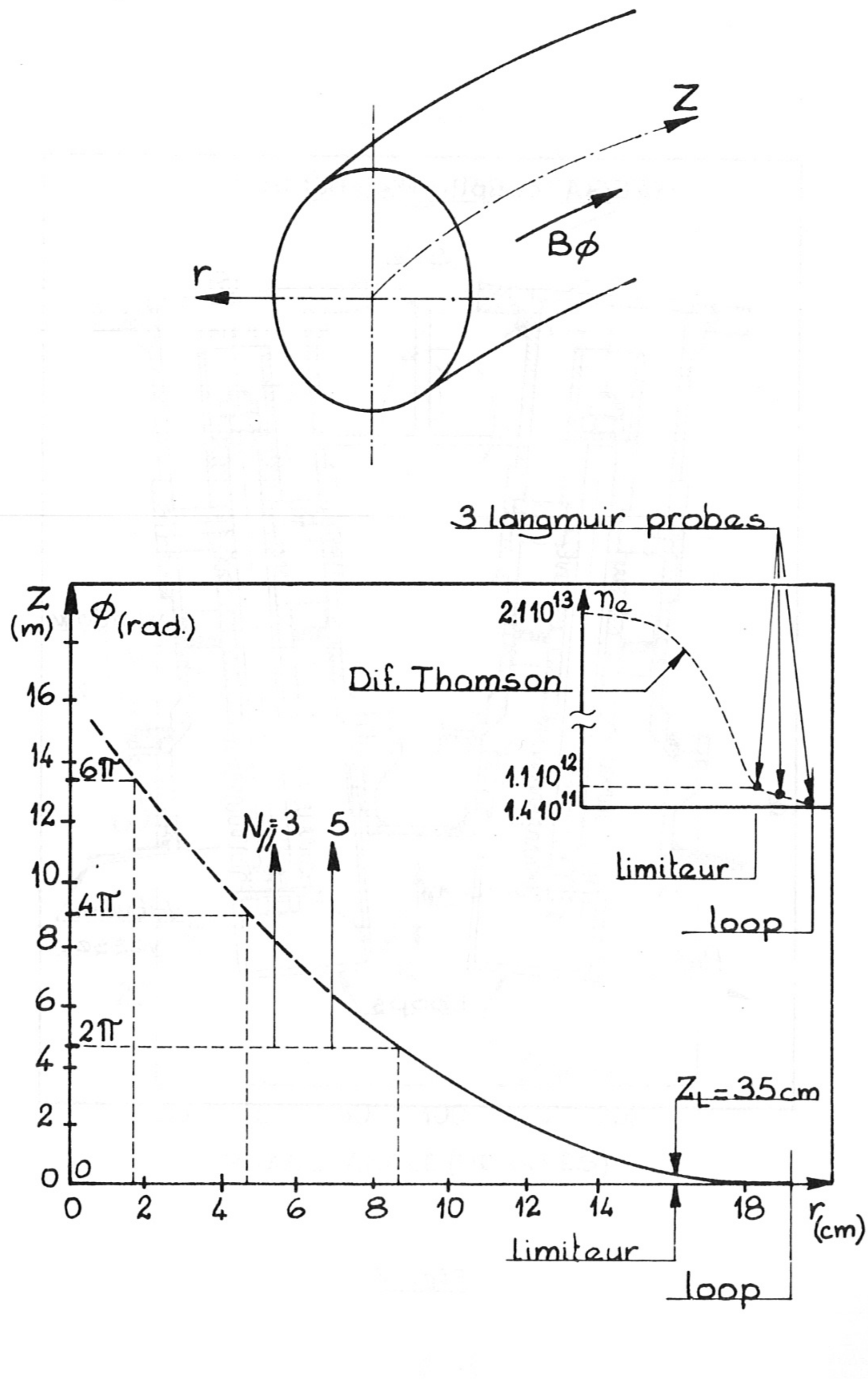

Z
Bφ
r
3 langmuir probes
Z (m)
φ (rad.)
2.1 10^13
n_e
Dif. Thomson
1.1 10^12
1.4 10^11
6π
4π
2π
N// = 3
5
limiteur
loop
Z_L = 35 cm
0
2
4
6
8
10
12
14
16
18
r (cm)
limiteur
loop

Fig. 4

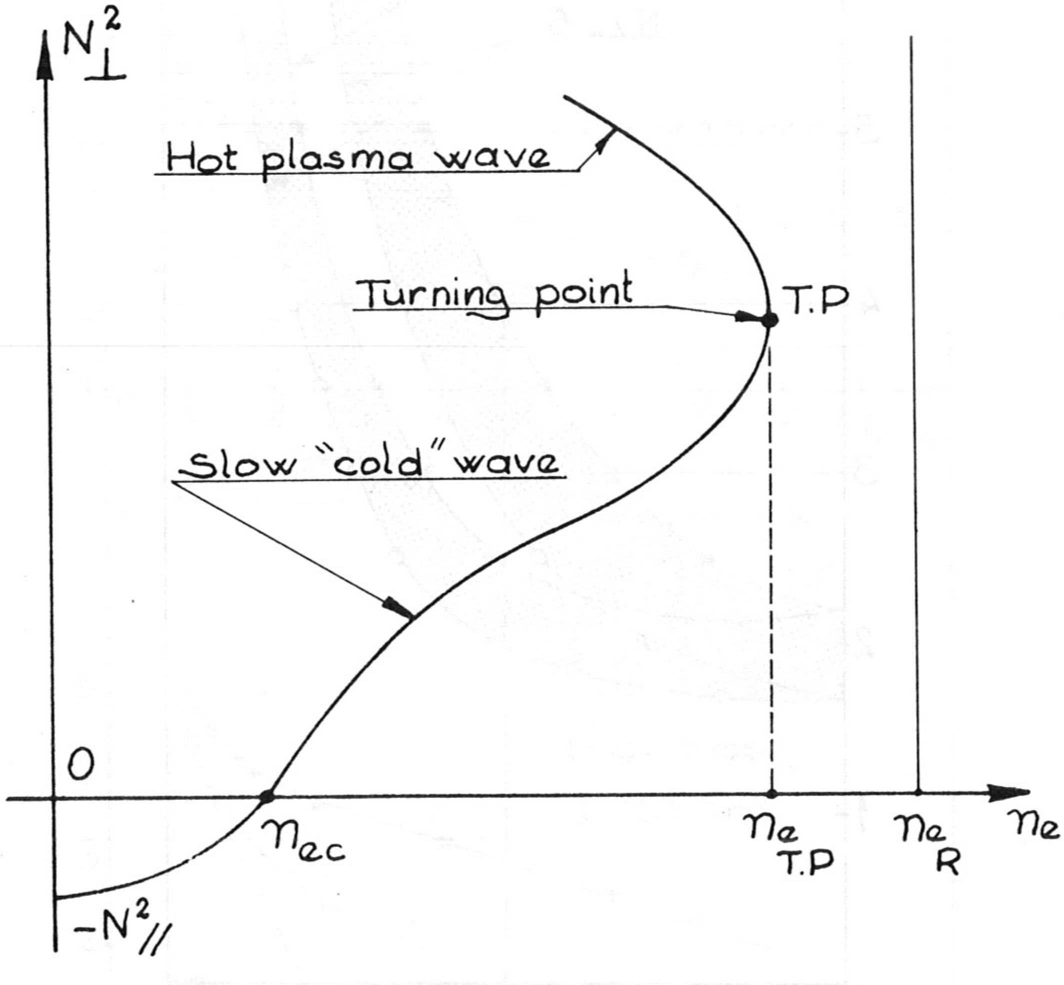

$N_\perp^2$
Hot plasma wave
Turning point
T.P
Slow "cold" wave
0
n_{ec}
$n_{e\,T.P}$
$n_{e\,R}$
n_e
$-N^2_{//}$

Fig. 5

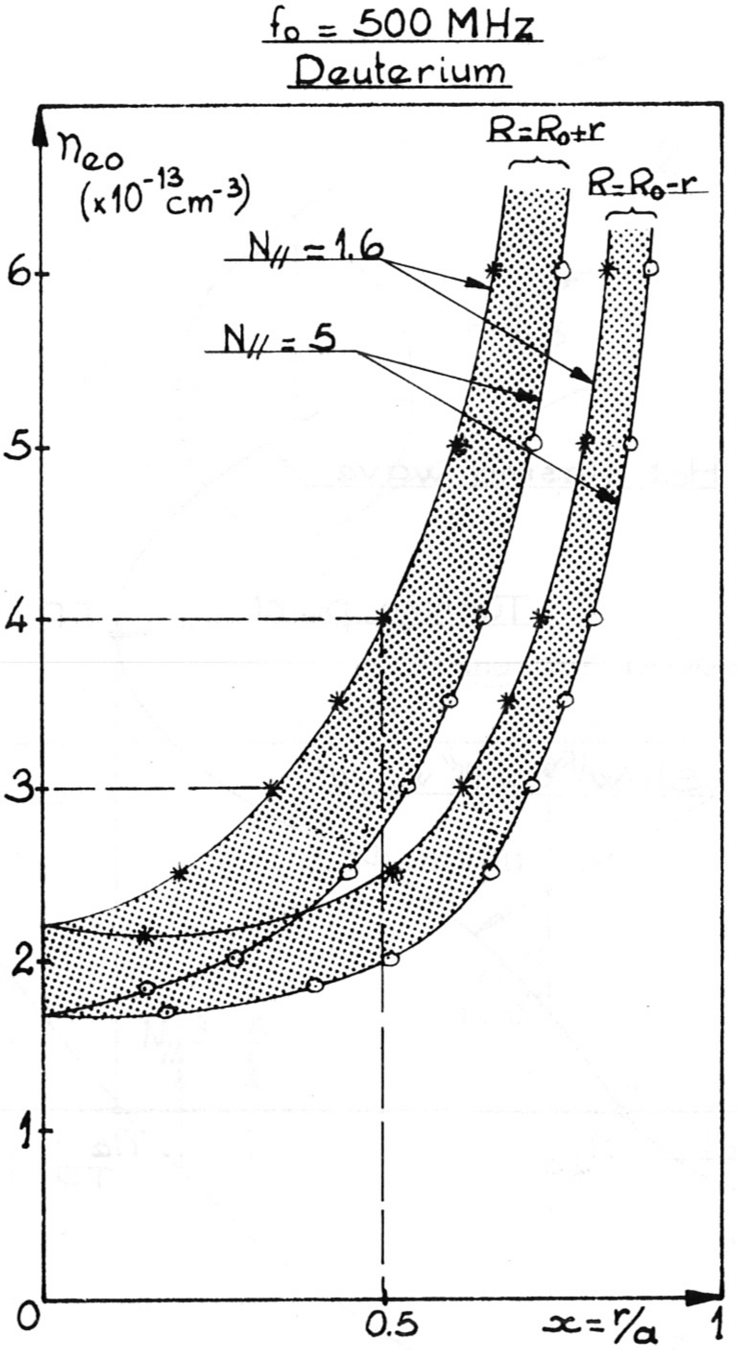

$$T_i = T_{io}\,(1-x^4) \rightarrow T_{io} = 150\,eV$$

$$n_e = n_{eo}\,(1-x^2)$$

$$B\phi = B\phi_o \frac{A}{A+x} \rightarrow B\phi_o = 14.4\,kG$$

Fig. 6

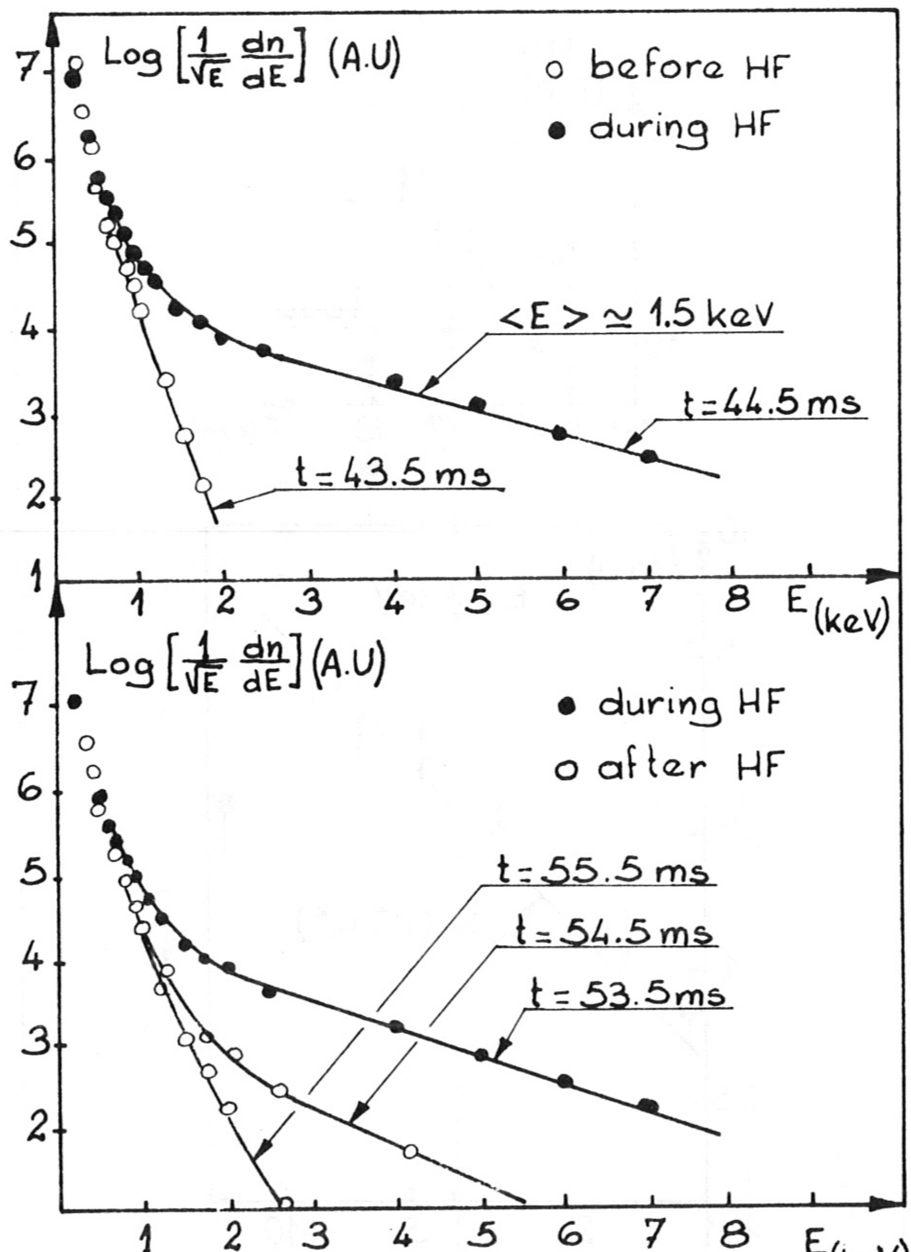

Log [1/√E dn/dE] (A.U)
o before HF
• during HF
<E> ≃ 1.5 keV
t=44.5 ms
t=43.5 ms
E (keV)
Log [1/√E dn/dE] (A.U)
• during HF
o after HF
t=55.5 ms
t=54.5 ms
t=53.5 ms
E (keV)

Fig. 7

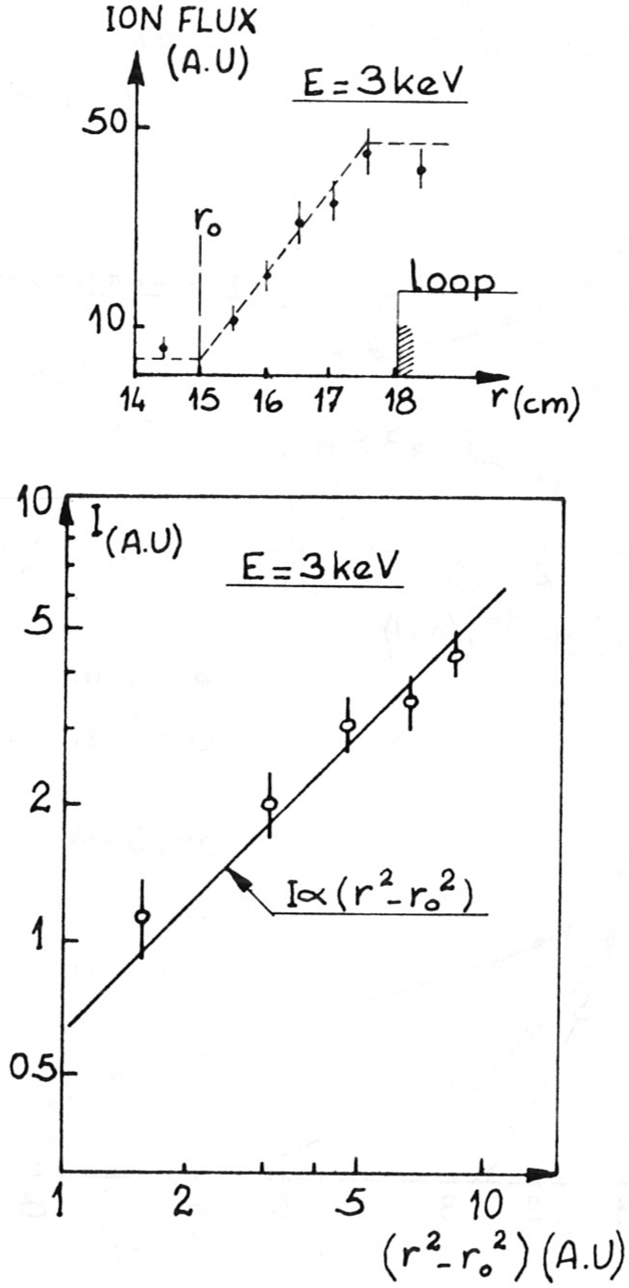
ION FLUX
(A.U)
E = 3keV
50
10
r_o
loop
14
15
16
17
18
r (cm)
10
I (A.U)
E = 3keV
5
2
1
0.5
I∝(r^2-r_o^2)
1
2
5
10
(r^2-r_o^2) (A.U)

Fig. 8

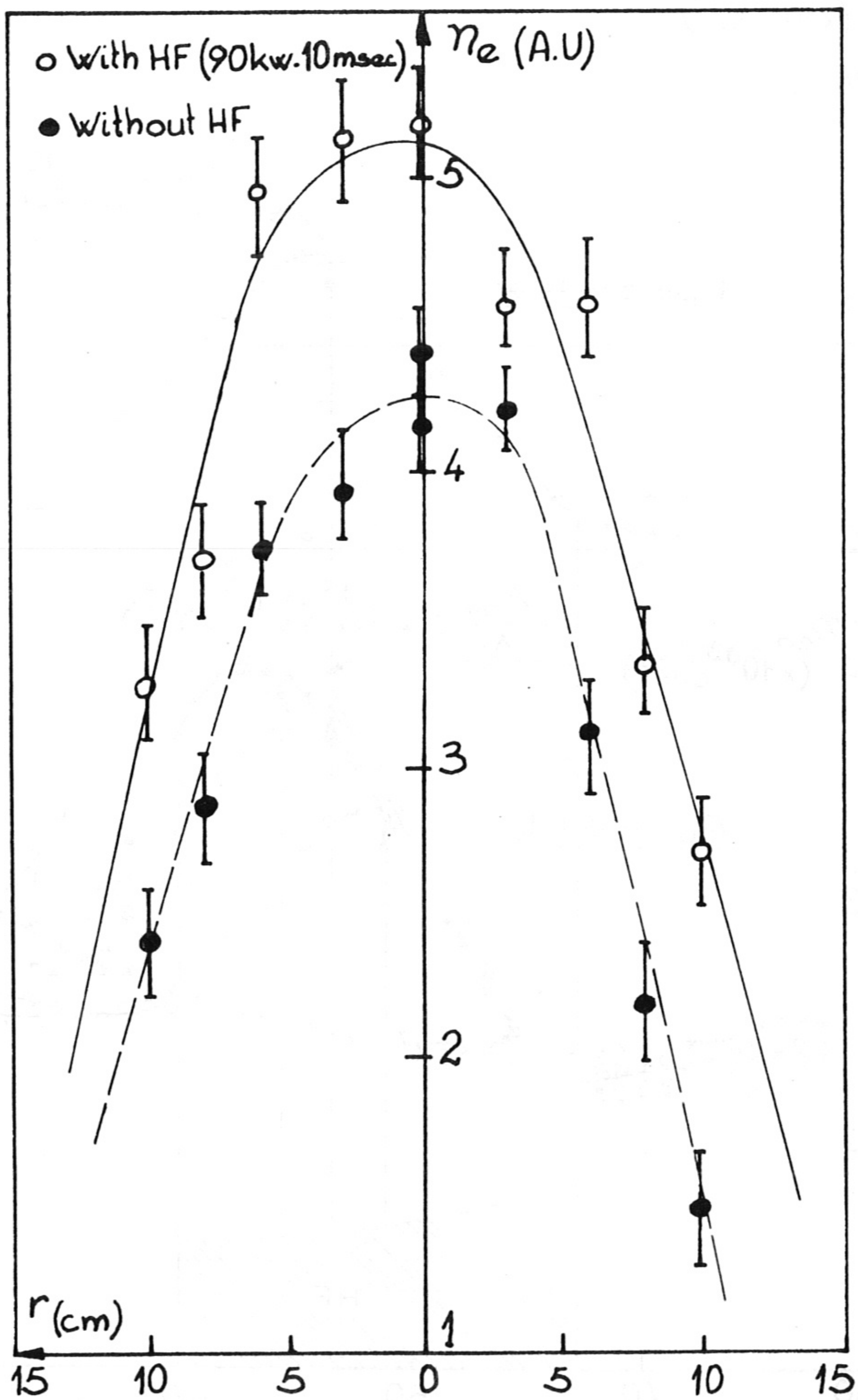

Fig. 9

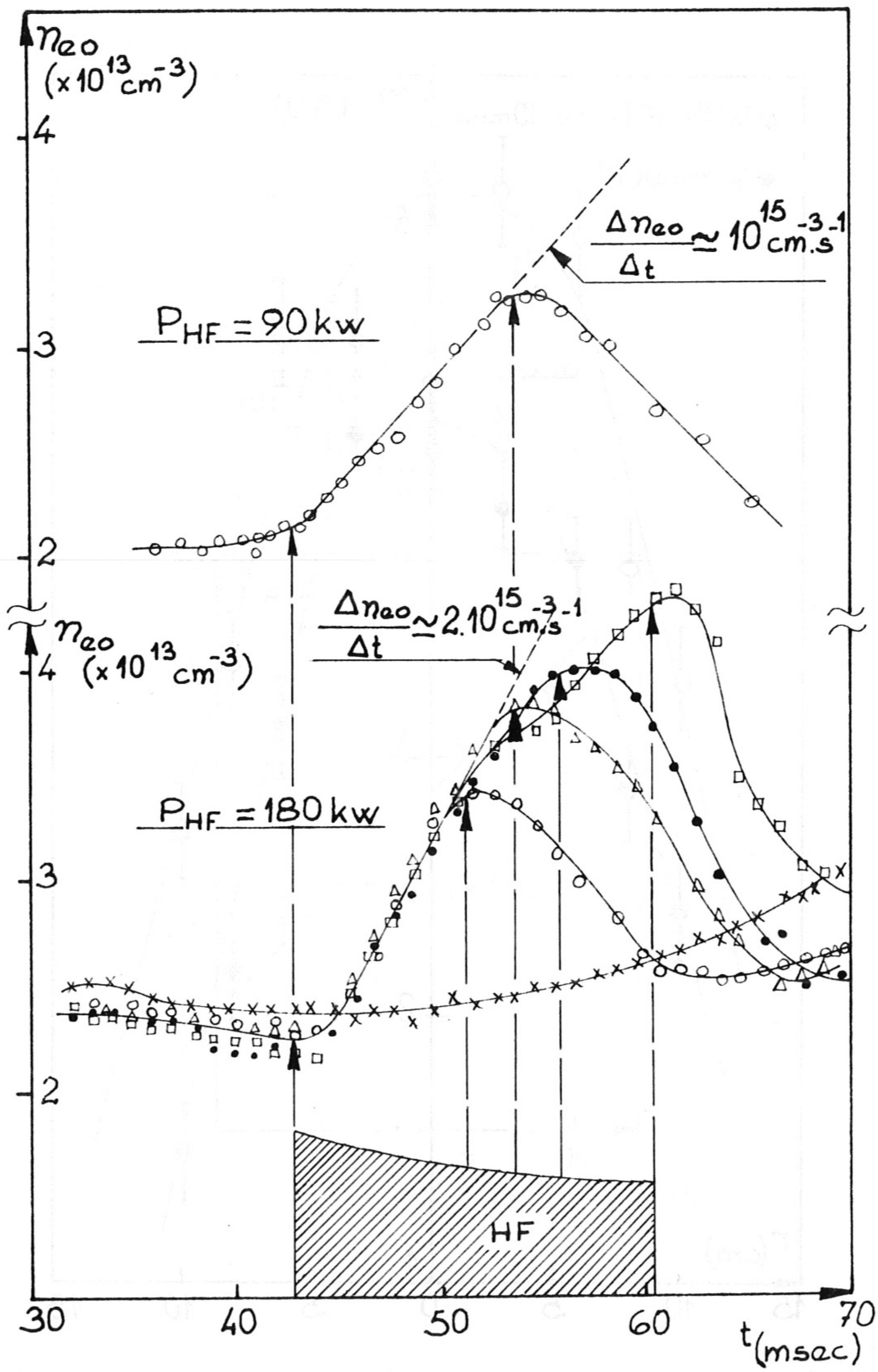

n_{eo} ($\times 10^{13}$ cm^{-3})
4
3
2
$\frac{\Delta n_{eo}}{\Delta t} \simeq 10^{15}$ cm^{-3}.s^{-1}
$P_{HF} = 90$ kw
n_{eo} ($\times 10^{13}$ cm^{-3})
$\frac{\Delta n_{eo}}{\Delta t} \simeq 2.10^{15}$ cm^{-3}.s^{-1}
$P_{HF} = 180$ kw
HF
30
40
50
60
70
t (msec)

Fig. 10

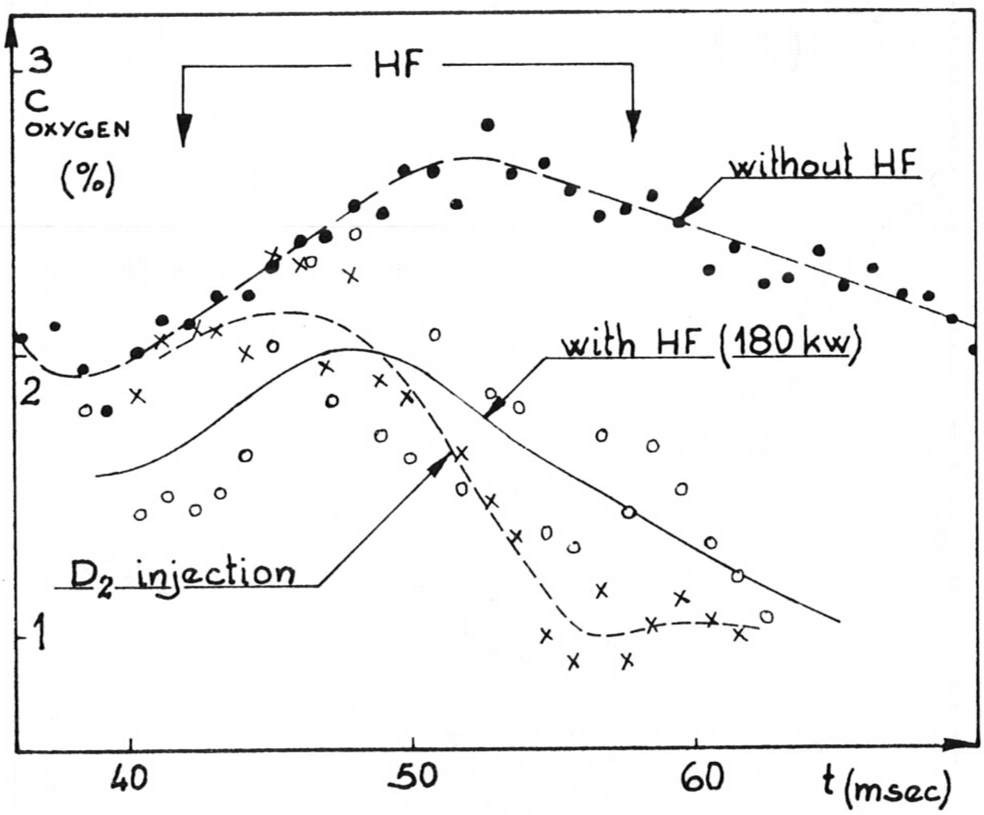
3
C
OXYGEN
(%)
HF
without HF
with HF (180 kw)
2
D2 injection
1
40
50
60
t (msec)

Fig. 11

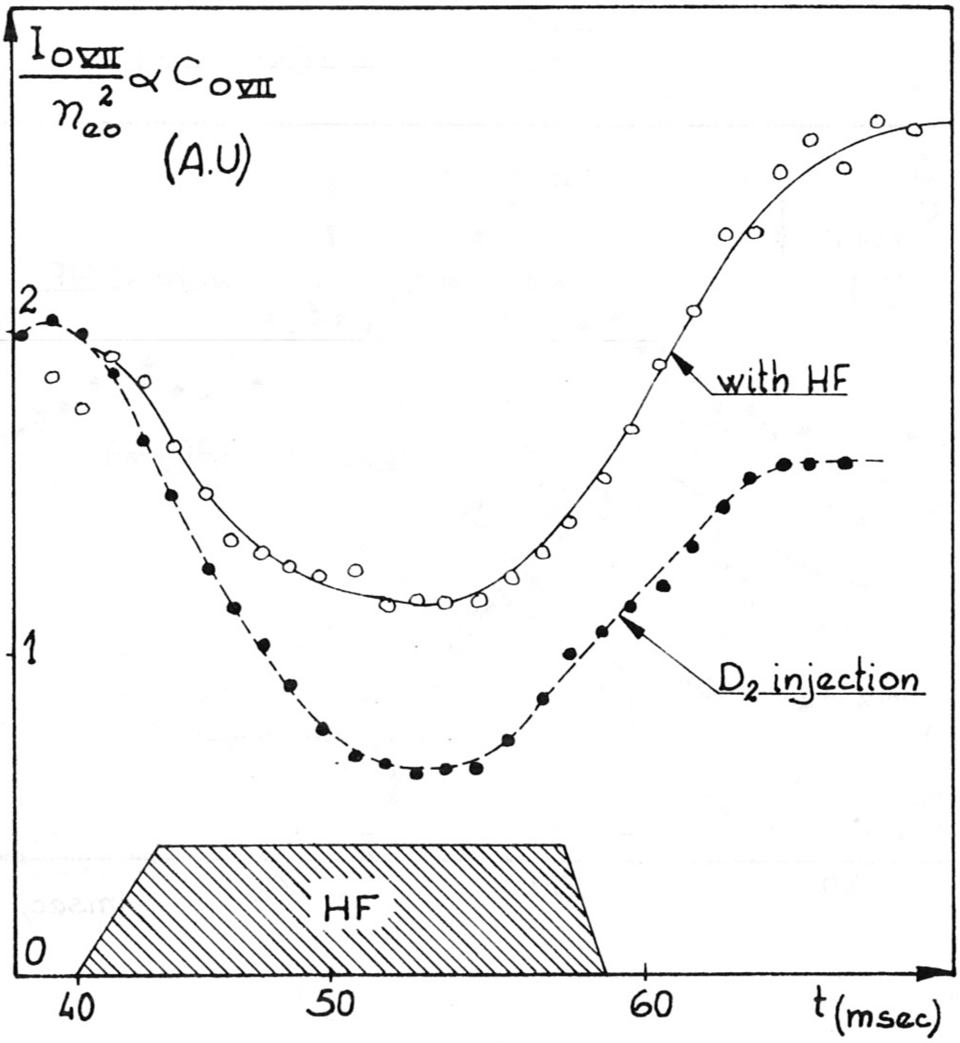

$\frac{I_{OVII}}{n_{eo}^2} \propto C_{OVII}$
(A.U)
2
1
0
with HF
D_2 injection
HF
40
50
60
t (msec)

Fig. 12

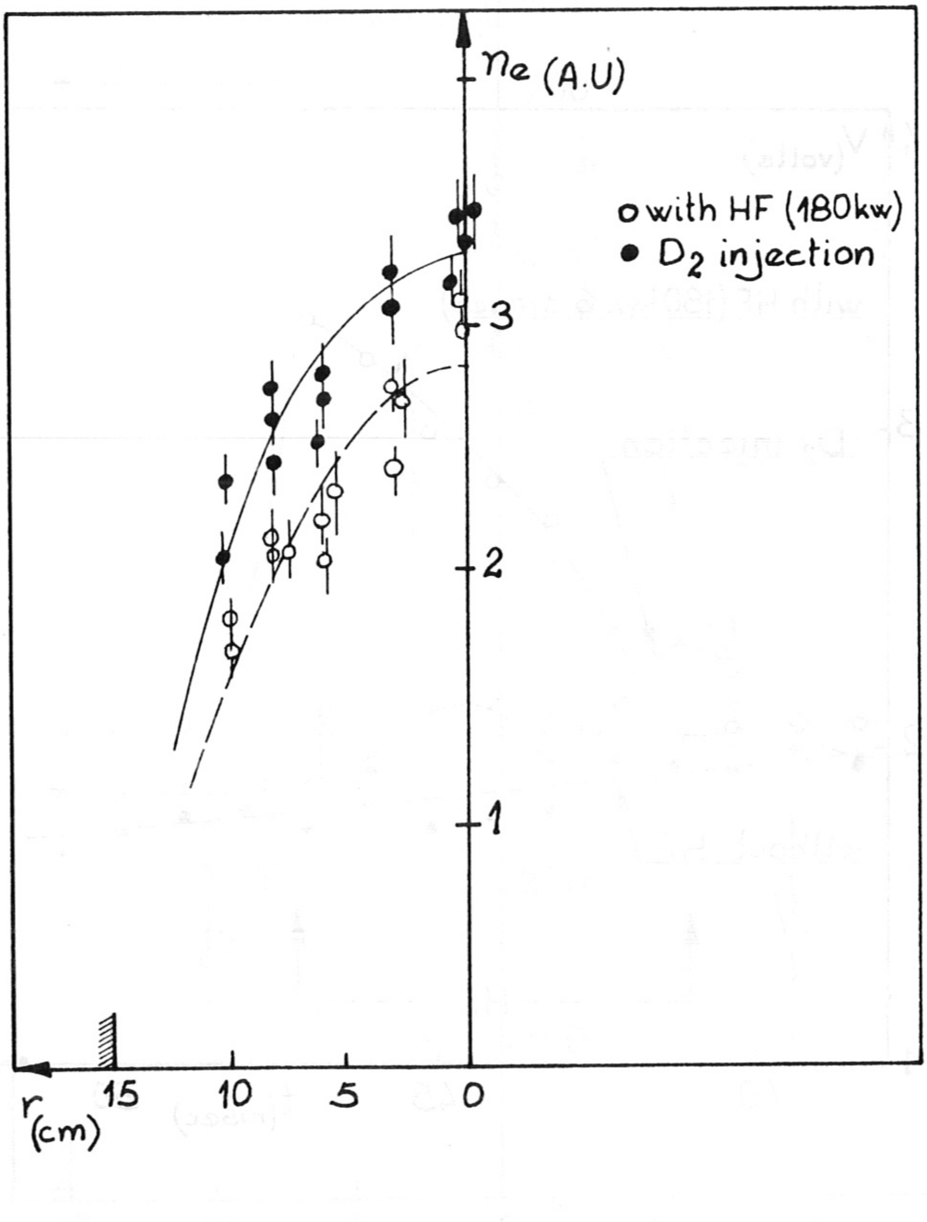

Fig. 13

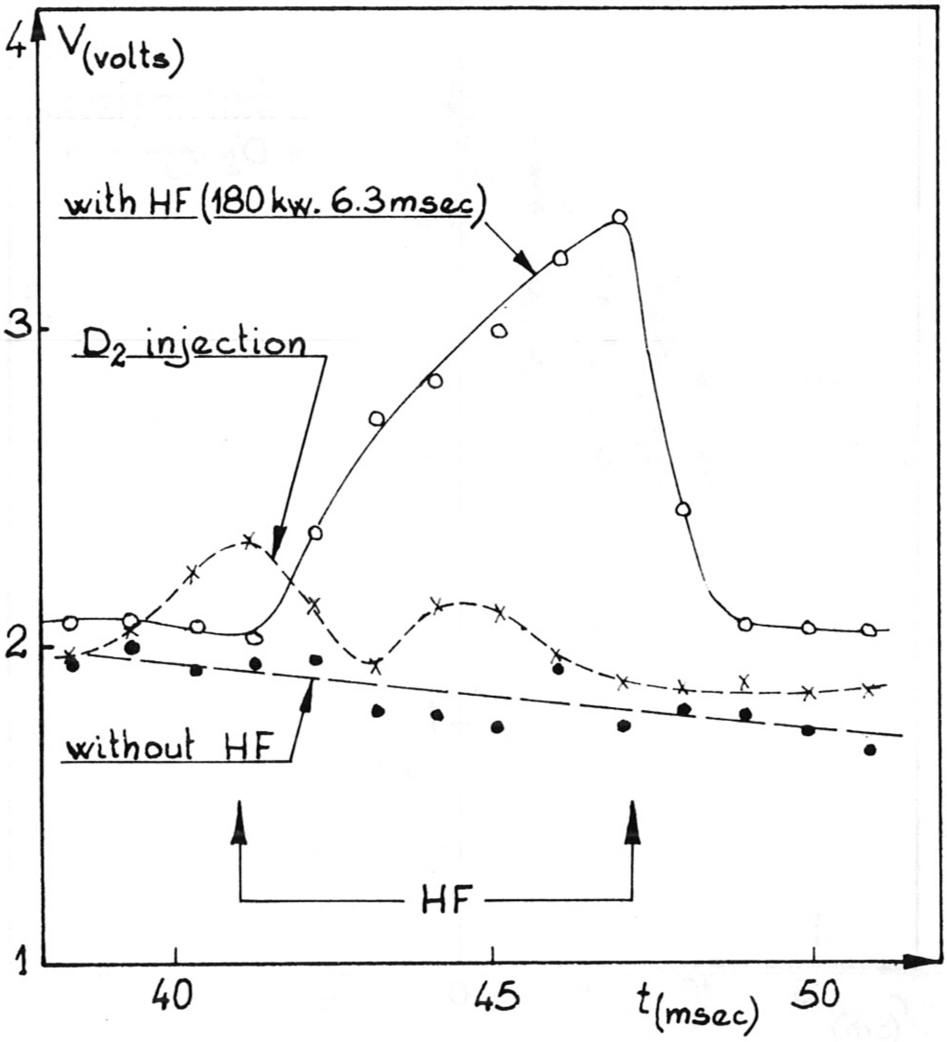

4
V(volts)
with HF (180 kw. 6.3 msec)
3
D2 injection
2
without HF
HF
1
40
45
t(msec)
50

Fig. 14

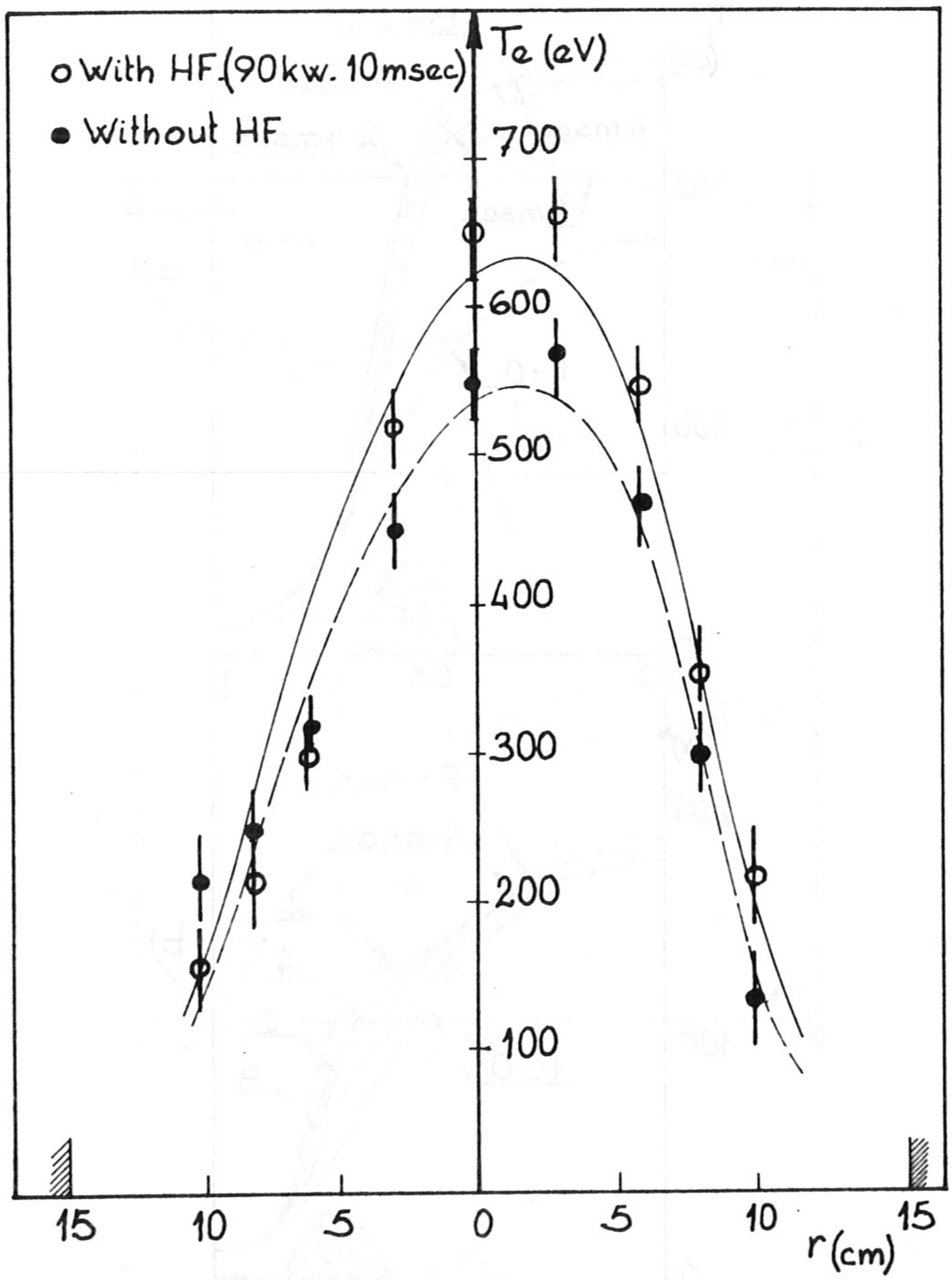
o With HF (90kw. 10msec)
• Without HF
T_e (eV)
700
600
500
400
300
200
100
15
10
5
0
5
10
15
r (cm)

Fig. 15

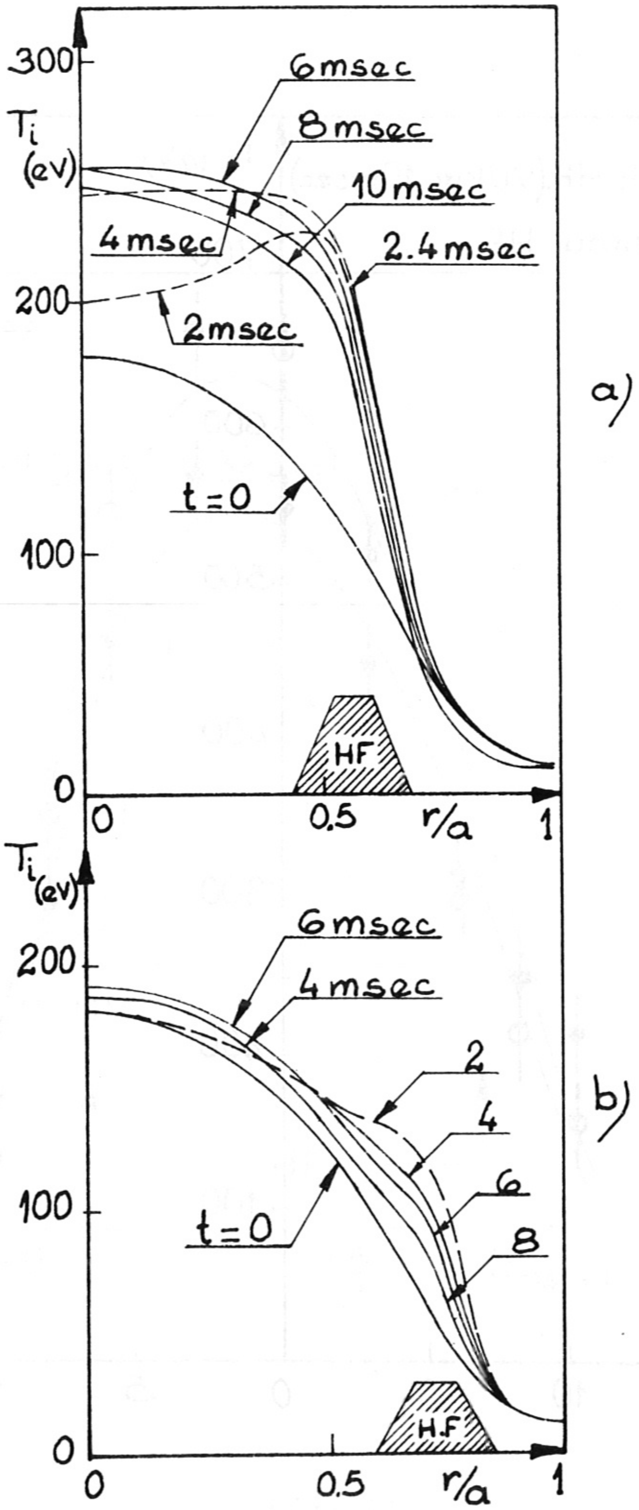

300
T_i (ev)
6 msec
8 msec
10 msec
4 msec
2.4 msec
200
2 msec
a)
t = 0
100
HF
0
0
0.5
r/a
1
T_i (ev)
6 msec
4 msec
200
2
4
b)
6
100
t = 0
8
H.F
0
0
0.5
r/a
1

Fig. 16

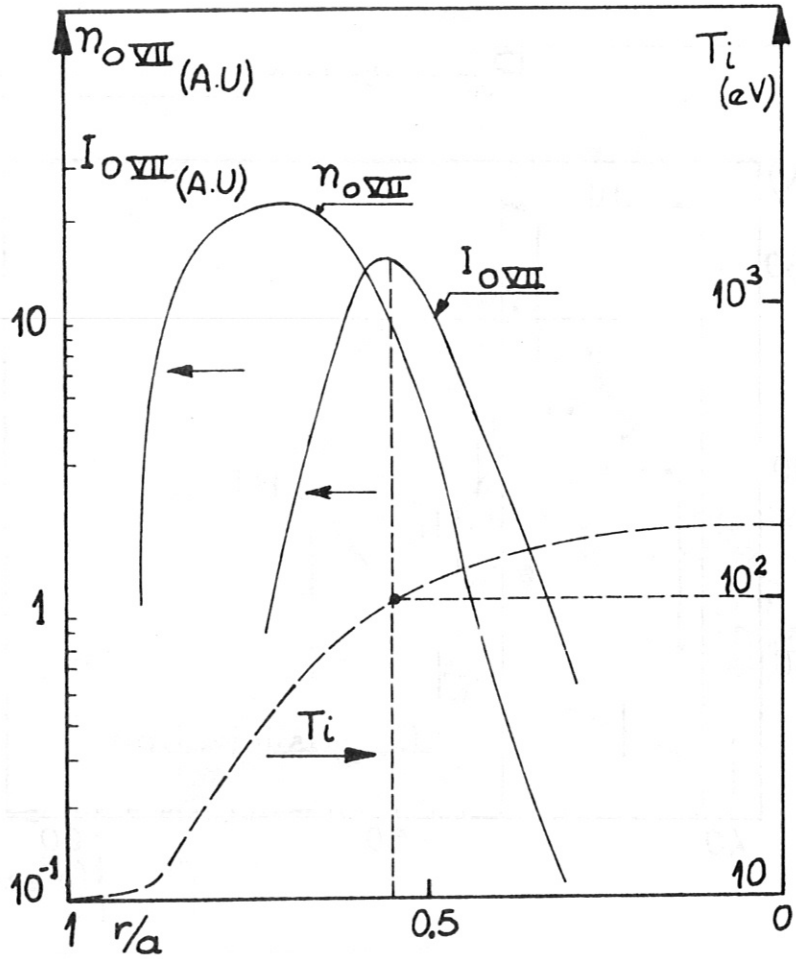

$n_{O\,VII}$ (A.U)
$I_{O\,VII}$ (A.U)
T_i (eV)
$n_{O\,VII}$
$I_{O\,VII}$
10
1
10^{-1}
10^3
10^2
10
Ti
1
r/a
0.5
0

Fig. 17

CHARGE - EXCHANGE MEASUREMENTS

$P_{HF} = 180$ kw

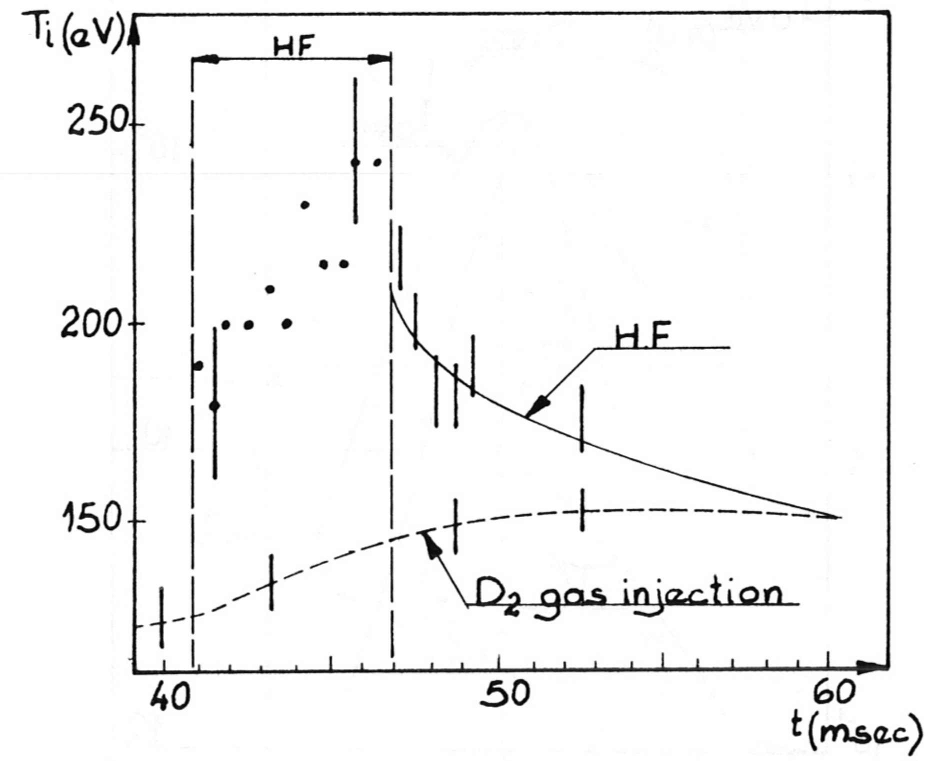

Fig. 18

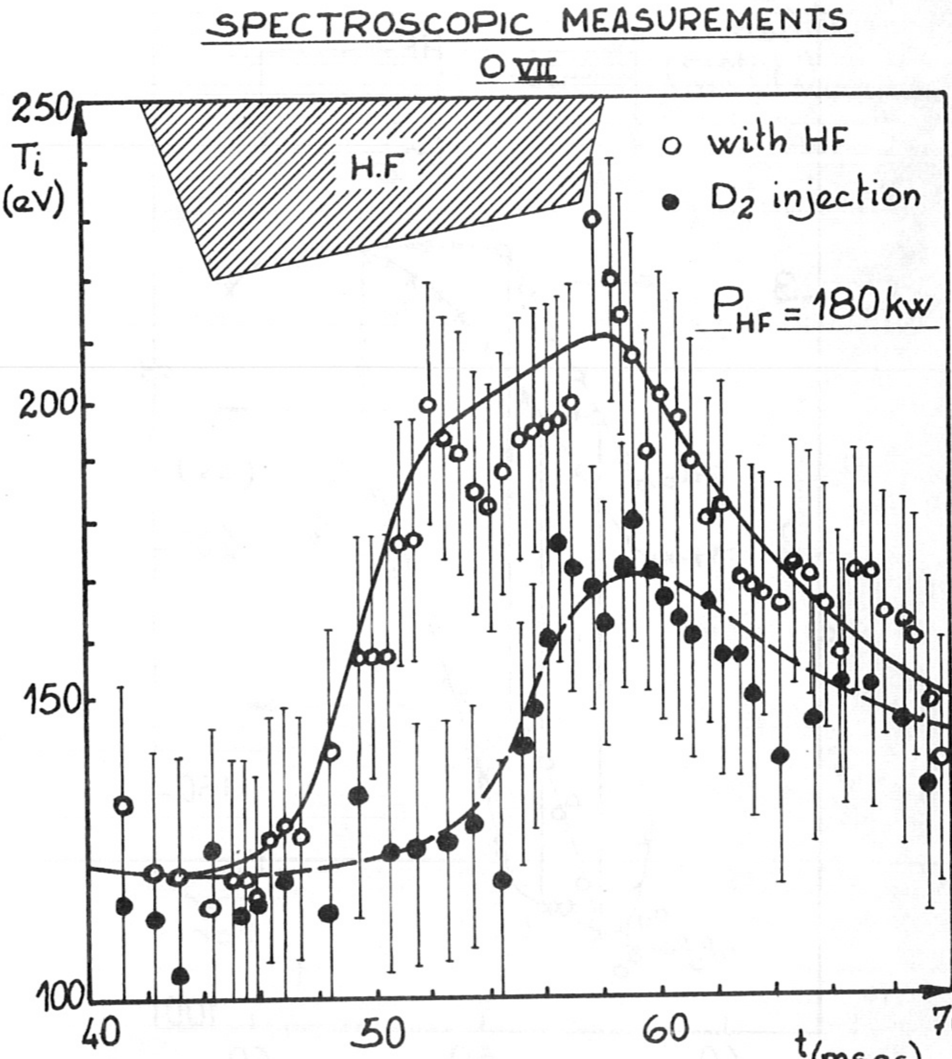

SPECTROSCOPIC MEASUREMENTS
O VII
250
T_i
(eV)
200
150
100
40
50
60
70
t (msec)
H.F
o with HF
• D_2 injection
P_{HF} = 180 kw

Fig. 19

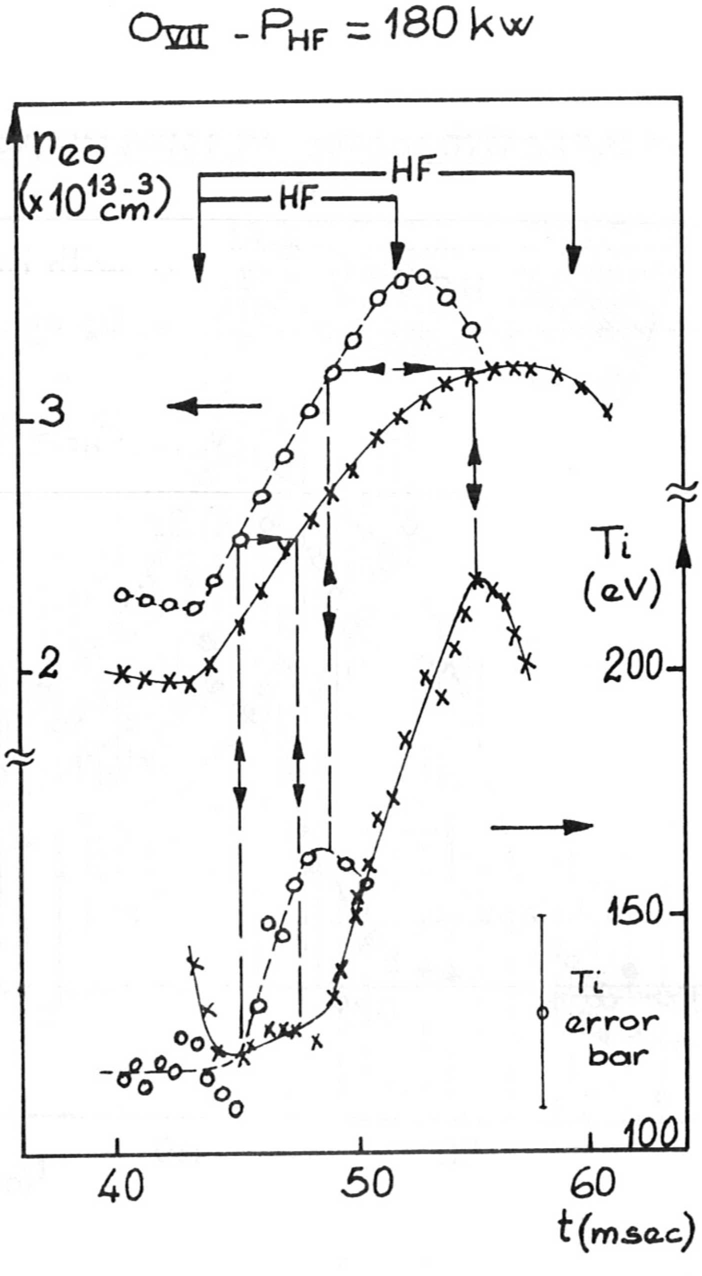

O_{VII} - P_{HF} = 180 kw
n_{eo} ($\times 10^{13}$ cm^{-3})
HF
HF
3
2
Ti (eV)
200
150
100
Ti error bar
40
50
60
t (msec)

Fig. 20